*hydrology*

MDPI

*Article*

# Multi-Objective Optimal Gate Control and Hydropower Scheduling of Haditha Dam Using the Improved Harris Hawks Multi-Objective (IMOHHO) Algorithm with Long Short-Term Memory (LSTM)

**Amer Salih [1,*], Qian Zhang [1], Alessandro Raschella [2], Ahmed Mohammed [1], Badr Abdullah [1], Yongqiang Qiu [1], Khalid Hashim [1], Omar Aldhaibani [2] and Mukesh Kumar Maheshwari [3]**

[1] School of Engineering and Built Environment, Liverpool John Moores University, Liverpool L3 3AF, UK; q.zhang@ljmu.ac.uk (Q.Z.); a.s.mohammed@ljmu.ac.uk (A.M.); b.m.abdullah@ljmu.ac.uk (B.A.); y.qiu@ljmu.ac.uk (Y.Q.); k.s.hashim@ljmu.ac.uk (K.H.)
[2] School of Computer Science and Mathematics, Liverpool John Moores University, Liverpool L3 3AF, UK; a.raschella@ljmu.ac.uk (A.R.); o.a.aldhaibani@ljmu.ac.uk (O.A.)
[3] Department of Electrical Engineering, Bahria University, Karachi Campus 75260, Pakistan; mukeshkumar.bukc@bahria.edu.pk
* Correspondence: a.m.salih@ljmu.ac.uk

## Abstract

Effective water management requires accurate forecasting of dam inflows, rainfall, and actual electricity demand. In this paper, we propose a framework for intelligent control of Haditha Dam gates using the improved Harris Hawks Multi-Objective algorithm (IMOHHO) with Long Short-Term Memory (LSTM). The study aims to develop a framework for scheduling the operation of the gates that strikes a balance between maximizing hydropower generation, maintaining storage levels close to the target value, reducing unused discharge, and optimizing the operations of the gates. This ensures that a minimum net head of a 147 m water level in the dam reservoir is maintained. The proposed model was applied to the Haditha Dam using operational gates and a 48-step time horizon with an interval of 30 min that could be changed as needed. In the IMOHHO-LSTM algorithm, each filtered solution represents an integrated timeline for the opening of the six gates throughout the runtime; the algorithm relies on the concept of non-dominant solutions and creates an archive of optimal solutions using the Pareto interface to achieve a balance between different operational objectives. The final results showed the potential of the proposed algorithm to ensure the efficient operation of the dam, with a total power generation of 10,434.14 MWh, while the average output power was 434.76 MW. The maximum capacity reached 660 MW, which represents the maximum design capacity of a modern dam. Furthermore, the model kept the storage level within a very narrow range of 2199 to 2206 $Mm^3$, centering around the target storage value of 2200 $Mm^3$. This confirms the passing of the IMOHHO-LSTM algorithm in balancing energy production with maintaining the operational requirements of the dam lake's water level.

**Keywords:** flow prediction; multiobjective optimization; harris hawks optimization (HHO); smart control for dam gates; LSTM

Check for updates

Academic Editors: Eliza Isabela Tică, Angela Neagoe, Bogdan Popa, Raquel López-Fernández and Emanuele Quaranta

Received: 11 September 2026
Revised: 21 October 2026
Accepted: 22 October 2026
Published: 29 October 2026

**Copyright:** © 2026 by the authors. Licensee MDPI, Basel, Switzerland. This article is an open access article distributed under the terms and conditions of the Creative Commons Attribution (CC BY) license.

## 1. Introduction

The global shift towards modern digital energy systems has increased the need for smart energy and water management strategies capable of achieving an effective balance between supply and demand [1]. These strategies must take into account the availability of seasonal water transition from the rainy season to the dry summer months in the Middle East [2], a period characterized by high energy demand for cooling and high water requirements for domestic use and agriculture [3]. Hydropower accounts for about 30% of global electricity consumption, a figure that continues to rise along with growing demand, increasing housing needs, and the growing need for green spaces to mitigate the effects of climate change [4,5]. In areas with distribution control, age control, and limited capacity infrastructure, the challenges of managing residential energy and water demand are becoming more acute [6]. These constraints, which are exacerbated by the nature of intermittent rainfall, high temperatures, and harsh climates, call for the adoption of advanced control strategies capable of improving the flow of energy and water in real time while maintaining the stability of water reserves [7].

Energy management systems have emerged as a vital enabling technology to address these challenges by coordinating the operation of distributed energy resources (DERs), water storage systems, and flexible electrical loads within residential environments [8–10]. The primary goal of these systems is to reduce electricity costs, improve water consumption, reduce grid demand at peak grid time, and improve overall energy efficiency, all while maintaining the convenience of residents [11,12]. However, the design and implementation of effective energy management systems face several interrelated challenges such as the random nature of factors affecting energy production, the difficulty of predicting water flows to the dam reservoir, the complexity of multi-objective optimization in the face of climate change uncertainty as illustrated in Figure 1, and the computational burden associated with real-time decision-making [13,14]. These challenges are exacerbated in regions facing extreme weather conditions, where it may be difficult to generate enough electricity from the grid during periods of peak demand, necessitating the adoption of more advanced and accelerated energy management strategies [15,16].

Historically, the systematic optimization of reservoir releases dates from the 1960*s*, when dynamic programming was first applied to the sequential decision structure of storage operation [17] and was extended through stochastic dynamic programming to account for inflow uncertainty [18]. Linear and nonlinear programming formulations of multi-reservoir systems followed [19], and comprehensive reviews of this period document both their strengths and the dimensionality barrier that limits them [20]. Practical tools built on these principles remain in operational use. But early methods of managing the energy generated in dams relied primarily on control strategies based on predetermined rules (inferences) [21] and threshold-based decision-making criteria for scheduling operations and managing the opening and closing of dam gates [22–24]. While rule-based methods are simple and interpretable, they have fundamental limitations that limit their effectiveness in dynamic and uncertain environments [25]. Rule-based controllers typically operate in an interactive manner, responding to current system states without anticipating future conditions or learning from historical patterns [26,27]. Immediate reactions lead to imperfect decisions, especially in scenarios involving the opening of dam gates variably over time [28], fluctuations in power generation, and ill-considered load patterns [29]. Furthermore, rule-based approaches lack the flexibility to adapt to changing environmental conditions and seasonal changes, requiring manual recalibration and expert knowledge for each specific deployment context [30].

Optimization-based approaches face significant practical challenges because they require precise mathematical models of the thermodynamics, behavior and properties

of climate change components that are often difficult to obtain, calculate or maintain in practical applications [31,32]. The computational complexities associated with solving large-scale optimization problems in real time can be prohibitive, especially when considering the combinatorial nature of hardware operation scheduling and the nonlinear dynamics of the systems. These methods exhibit limited generalization capabilities, as they struggle to handle the volatility of energy sources [33]. Machine learning and artificial intelligence technologies have gained significant momentum in energy management research during the past decades [34], providing the ability to overcome many of the shortcomings of traditional methods [35]. Recent comprehensive studies on computational intelligence approaches to energy management systems (EMSs) have been reviewed, highlighting challenges related to feasibility, specificity, and practicality on the ground.




**Figure 1.** The difference in water flow between winter and summer at the Haditha Dam: (**a**,**c**) for winter, and (**b**,**d**) for summer.

Among the various machine learning models, supervised learning methods stand out including recurrent neural networks (RNNs) and Long Short-Term Memory (LSTM) networks [36]. Accurate forecasting is essential for efficient energy management, as it can inform proactive scheduling decisions and mitigate the uncertainty inherent in energy systems [37]. Advanced architectures combining multi-objective forecasting and scheduling have shown significant operational and environmental benefits [38,39], while climate adaptation frameworks have combined hybrid forecasting algorithms and multi-objective optimization to address system-level challenges. Recent studies indicate that deep learning architectures can achieve higher prediction accuracy compared to traditional statistical

methods [36]. However, most existing approaches treat prediction and control as separate tasks, and we aim to integrate them as coherent components within a unified decision-making framework. Because of that, predicting water flow into rivers is an essential part of clean hydropower generation, and it is important from economic, social and environmental perspectives [40]. We investigated the feasibility of real-time energy management and self-forecasting using the hybrid model (GA-LSTM) through a previous case study, and a paper on this topic is published here [41].

This research paper proposes a new framework based on the IMOHHO-LSTM model for smart energy management in regions with limited generation capacity, addressing existing research gaps through several key contributions. First, the framework integrates dam inflow forecasting techniques using artificial neural networks, enabling proactive decision-making based on accurate predictions of future load and generation patterns. It also maintains dam reservoir water levels to achieve economic objectives while simultaneously improving environmental outcomes. Data mining techniques are employed to analyze energy consumption across daily, weekly, and monthly timescales, providing precise insights into consumption patterns and allowing for the implementation of targeted control measures. Furthermore, the framework optimizes dam gate operations based on time-dependent energy demand; this enhances economic performance and balances short-term water usage with storage for dry seasons, thereby ensuring long-term system stability. Finally, the framework implements strategies to mitigate the impact of unexpected peak energy demand by forecasting future demand patterns and proactively scheduling flexible operations, thereby managing reservoir depletion during peak periods. The proposed approach was evaluated using real-world data, demonstrating superior performance across multiple metrics compared to rule-based methods, optimization-based approaches, and traditional deep learning techniques, including two previously studied models.

The rest of this paper is organized as follows: In Section 2, the study was reviewed by identifying the study area and data sources to ensure the accuracy of the inputs. Then, in Section 3, we move to the heart of the work with the proposed methodology, which is based on building an intelligent model that combines an LSTM network for accurate prediction of temporal data and the improved Harris Hawks Multi-Objective algorithm (IMOHHO) to improve operating decisions. It is planned that this hybrid model will be applied in simulating the operation of the dam. The results are then presented and discussed in Section 4, which covers performance analysis of the gates, storage levels and generated power as well as Pareto front analysis to balance conflicting objectives. The study concludes by discussing the efficiency of the algorithm compared to others in Section 5, leading to the conclusions of Section 6 that summarize the effectiveness of the model in optimally managing water and electrical resources.

## 2. Study Area and Data Sources

Haditha Dam was chosen as the case study area. Haditha Dam is located on the Euphrates River in Anbar Governorate, western Iraq, near the city of Haditha, as illustrated in Figure 2. Haditha Dam is considered one of the most important water and hydroelectric facilities in Iraq [42]. The goal of establishing the dam was to achieve a set of strategic functions, including regulating the flow of the Euphrates River, providing water for various uses, and producing electrical energy through a hydroelectric station. The dam is located within an area characterized by an arid to semi-arid climate. The Haditha Dam reservoir is one of the largest operating reservoirs in Iraq, and it plays an important role in balancing water resources between periods of water abundance and periods of drought. In terms of engineering specifications, the Haditha Dam is a large dam equipped with a hydroelectric power generation system. It is about 57 m high (or the top of the dam is 154 m above sea

level) and extends for about 9 km. The dam includes a hydropower plant containing six Kaplan turbines with a total design capacity of 660 MW (Table 1).




**Figure 2.** Location of the Haditha Dam at the Euphrates River (Iraq) [41].

**Table 1.** Haditha Dam physical characteristics and operational constraints.

| System Parameter | Value/Unit | Physical Meaning/Constraint |
|---|---|---|
| Scheduling horizon | 24 h | Total flood operation timeframe |
| Time resolution ($\Delta t$) | 30 min | Step duration (48 distinct control intervals) |
| Number of spillway gates | 6 | Individually controlled radial gates |
| Initial reservoir storage ($S_0$) | $6.0 \times 10^9$ m$^3$ | Starting water storage volume |
| Maximum allowable storage ($S_{max}$) | $8.2 \times 10^9$ m$^3$ | Flood control crest limitation |
| Minimum conservation storage ($S_{min}$) | $2.5 \times 10^9$ m$^3$ | Ecological and intake requirement |
| Max individual gate capacity ($q_{max}$) | 1333.3 m$^3$/s | Max discharge per gate (8000 m$^3$/s total) |
| Turbine release capacity ($Q_{turb}$) | 1200 m$^3$/s | Fixed maximum power generation discharge |
| Max gate movement speed ($\Delta u_{max}$) | 0.90/step | Max 90% opening adjustment per 30 min |

The hydraulic system also includes gates for drainage control and a system for drainage of excess water to handle water flows during periods of flooding. The reservoir is the main element of this process, as the water level inside is controlled based on the volume of flows and the amount of water that is discharged through the gates and turbines. The equation of the water balance of the water reservoir can be expressed as follows:

$$S_{t+1} = S_t + (Q_{in,t} - Q_{out,t} - Q_{spill,t})\Delta t \quad (1)$$

where $S_t$ represents the storage volume at time $t$, $Q_{\text{in},t}$ represents the inflow to the reservoir, $Q_{\text{out},t}$ represents the discharge used for power generation or control, and $Q_{\text{spill},t}$ represents the spill discharge resulting from floods or from exceeding the operational capacity. In this paper, a modern dam representation involving the use of six operational gates ($Ng = 6$) is proposed, where the variables represent the amount of opening of each gate in each time step. The operating matrix can be defined as follows:

$$X = \begin{bmatrix} G_{1,1} & G_{2,1} & \dots & G_{6,1} \\ G_{1,2} & G_{2,2} & \dots & G_{6,2} \\ \vdots & \vdots & \ddots & \vdots \\ G_{1,T} & G_{2,T} & \dots & G_{6,T} \end{bmatrix} \quad (2)$$

where $G_{i,t}$ represents the ratio of gate opening $i$ at time $t$. The gate opening is limited within the range:

$$0 \leq G_{i,t} \leq 100 \tag{3}$$

where a value of $G_{i,t}$ = 0 means that the gate is completely closed, while a value of $G_{i,t}$ = 100 means that it is fully open. The outflow from each gate was calculated using the flow through the flow equation:

$$Q_i = C_d A_i \sqrt{2gH} \tag{4}$$

where $Q_i$ is the rate of discharge through the gate $i$, $C_d$ is the discharge coefficient, $A_i$ is the effective aperture area, and $H$ is the hydraulic height (hydraulic pressure). The aperture area is calculated as follows:

$$A_i = W_g O_i \tag{5}$$

where $W_g$ is the gateway width and $O_i$ is the opening ratio. So the total discharge should be:

$$Q_{total} = \sum_{i=1}^{N_g} Q_i \tag{6}$$

The hydraulic head height is one of the most important variables affecting energy production. At the Haditha Dam, this height does not remain constant, but changes depending on the level of storage as follows:

$$H_t = f(S_t) \tag{7}$$

where $22 \leq Ht \leq 46$ m, depending on the level of the water reservoir. In the simulation model, we used the parameters illustrated in Table 2.

**Table 2.** Water levels and net hydraulic head of Haditha Dam.

| Condition | Upstream Level (m a.s.l) | Net Head $H_t$ (m) |
|---|---|---|
| Target Head Operation | 147.0 | 41.7 |
| Maximum Flood | 150.2 | 45.9 |
| Minimum Operation | 129.5 | 22.2 |
| Dead Storage | 112.0 | 4.7 |

To calculate the electrical power produced which depends on the discharge rate, hydraulic head height and turbine efficiency, we use the following:

$$P_t = \eta \rho g Q_t H_t \tag{8}$$

The following is used change to MW:

$$P_{MW} = \frac{\eta \rho g Q_t H_t}{10^6} \tag{9}$$

where $\eta = 0.9$ hydropower is the system efficiency, $\rho = 1000$ kg/m$^3$ is the water density, and $g = 9.81$ m/s$^2$ is the acceleration due to gravity. Table 3 summarizes all the agreement models used in the IMOHHO algorithm.

Figure 3 shows that the real data collected cover at least two and a half years at 15 min intervals, between 2022 and 2024, around Haditha Dam. All of them were used to include input variables for the LSTM considering the following split: 70% training, 15% validation, and 15% testing. The following variables were used in modeling:

- (Maximum, minimum, and average) Atmospheric pressure (Pa);

- (Maximum, minimum, and average) Air temperature (°C);
- (Maximum, minimum, and average) Wind speed (km/h);
- (Maximum, minimum, and average) Relative humidity (%);
- Historical dam inflow ($m^3/s$);
- Upstream water level (m);
- Water discharge rate ($m^3/s$);
- Net head (m);
- Electrical energy produced (MWh);
- Downstream water level (m).

**Table 3.** All the agreement models used in Haditha Dam.

| Parameter | Value |
|---|---|
| Number of Gates | 6 |
| Time Step | 1800 s |
| Simulation Horizon | 48 steps |
| Target Storage | 2200 $Mm^3$ |
| Maximum Storage | 2500 $Mm^3$ |
| Minimum Storage | 1500 $Mm^3$ |
| Gate Width | 8 m |
| Gate Height | 6 m |
| Discharge Coefficient | 0.68 |
| Efficiency | 0.90 |
| Maximum Power | 660 MW |
| Real Daily Data | 18 variables |




**Figure 3.** Actual daily data for Haditha Dam and related details.

## 3. Proposed Methodology

This paper proposes an intelligent framework for the optimal operation of Haditha Dam gates using the IMOHHO-LSTM algorithm. The proposed framework combines a hydraulic simulation model and an evolutionary optimization algorithm to determine the optimal operating schedule for the gates, with the goal of maximizing hydropower generation while maintaining reservoir stability and minimizing operational risks. The proposed system consists of four main phases: reading the flow data, generating initial gate operating solutions, evaluating each solution using a hydraulic simulation model, and optimizing the solutions using the IMOHHO algorithm.

### *3.1. LSTM Model Architecture*

LSTM networks represent a paradigm shift and a fundamental development in the field of deep learning, especially with regard to processing sequential and temporal data. Unlike traditional RNNs, which suffer from the vanishing gradient problem when dealing with long sequences, LSTM systems come with an innovative mechanism based on three main control gates, the forget gate, the input gate, and the output gate, in parallel with the cell state, which acts as a long-term memory capable of retaining relevant information

over long periods of time [43]. Figure 4 shows that the LSTM cell is governed by the following equations:

$$f_t = \sigma\left(W_f \cdot [h_{t-1}, x_t] + b_f\right) \quad (10)$$

$$i_t = \sigma(W_i \cdot [h_{t-1}, x_t] + b_i) \quad (11)$$

$$\tilde{C}_t = \tanh(W_C \cdot [h_{t-1}, x_t] + b_C) \quad (12)$$

$$C_t = f_t.C_{t-1} + i_t.\tilde{C}_t \quad (13)$$

$$o_t = \sigma(W_o.[h_{t-1}, x_t] + b_o) \quad (14)$$

$$h_t = o_t.\tanh(C_t) \quad (15)$$

In these equations $f_t$, $i_t$, $\tilde{C}_t$, $C_t$, $o_t$, and $h_t$ denote the forget gate, input gate, candidate cell state, cell state, output gate, and hidden state, respectively. The matrices $W_f$, $W_i$, $W_c$, and $W_o$ represent the weight matrices associated with the forget gate, input gate, candidate cell state, and output gate, respectively. Similarly, $b_f$, $b_i$, $b_c$, and $b_o$ denote the corresponding bias vectors. The function $\sigma(\cdot)$ represents the sigmoid activation function, while $[\tanh(\cdot)]$ denotes the hyperbolic tangent activation function.

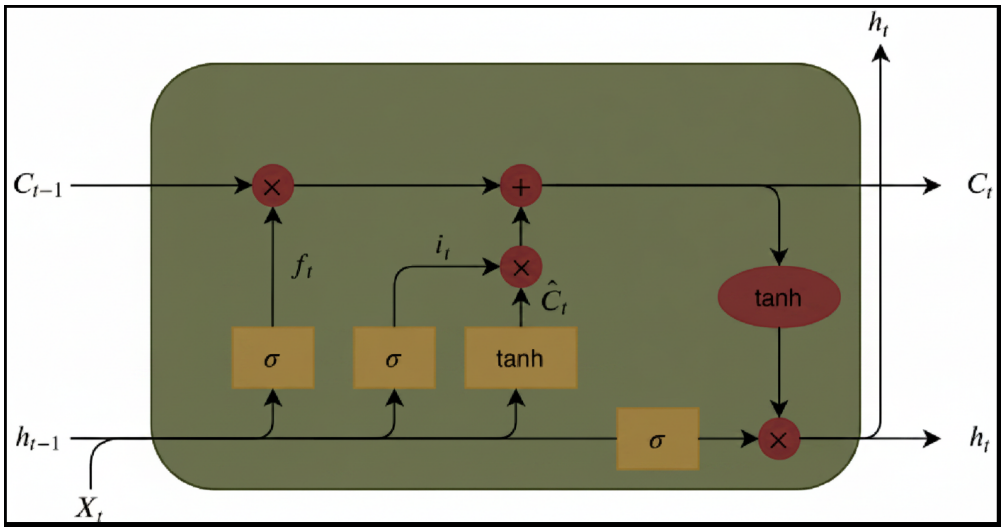



**Figure 4.** LSTM architecture.

Figure 5 shows that iteratively serializing LSTM layers enables the model to learn more complex and deeper representations of sequential data, with each layer extracting features at a higher level of abstraction than the previous layer. In other words, the first layer captures simple and straightforward temporal patterns in the data, while the deeper layers discover more complex and abstract temporal relationships and dependencies, greatly improving the predictive performance of the model. In parallel, the unit maintains the cell state which represents the long-term memory of the network, and this state is transmitted through successive recurrent units loaded with essential information that the gates have decided must be preserved. The true genius of this structure is evident in its ability to select information with great accuracy. The symbol $x_t$ in the figure represents the input data at time $t$ and $h_{t-1}$ represents the hidden layer output at time $t-1$, while $c_{t-1}$ represents the state of the cell at time $t-1$, $c_t$ represents the state of the cell at time $t$, and $\sigma$ refers to the sigmoid function. The values of the output $h_t$ and the state of the cell $c_t$ at the current time are determined based on the value of the input $x_t$ at the current time, the output of the hidden layer at the previous time $h_{t-1}$, and the previous state of the cell $c_{t-1}$ [44]. This prevents the vanishing or exploding gradients of information over time. This robust architecture has proven its superior ability in multiple application fields such

as time series prediction, natural language processing, and complex pattern recognition, which has established the position of LSTM networks as one of the most prominent and reliable models in the frontier deep learning system.

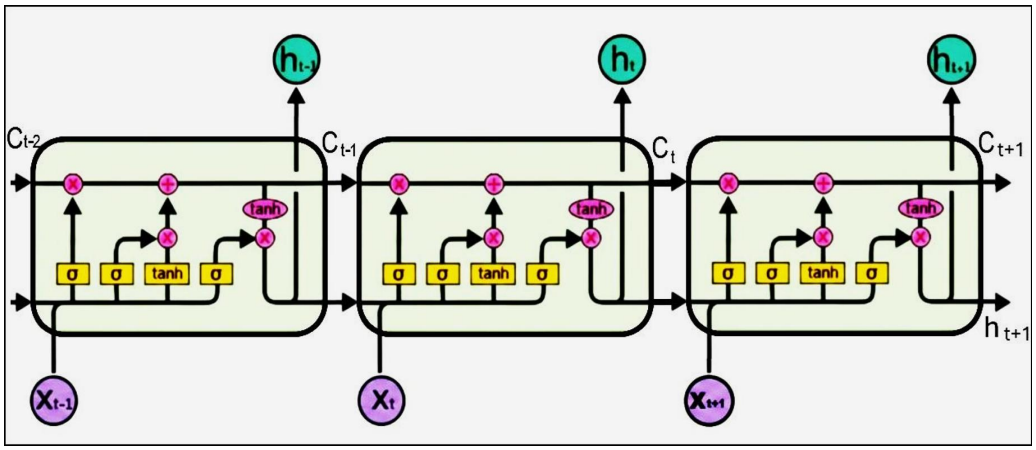



**Figure 5.** The repeating LSTM module for more complex and deeper representations.

### *3.2. Implemented LSTM Configuration*

The description above is generic; the configuration actually used in this study is given in Table 4. The hyperparameters marked as searched were selected by the HHO wrapper described in Section 3.3 using the validation partition only, with the mean squared error on that partition as the search objective. The remaining settings were fixed a priori.

**Table 4.** Architecture and training configuration of the implemented LSTM model. "Searched" indicates hyperparameters tuned by the HHO wrapper on the validation partition; the final column gives the selected value.

| Setting | Search Range | Selected |
|---|---|---|
| Number of LSTM layers | $\{1, 2, 3\}$ | L |
| Hidden units per layer | $[16, 128, 256]$ | U |
| Dropout rate | $[0.0, 0.5]$ | d |
| Learning rate | $[10^{-4}, 10^{-2}]$, log scale | lr |
| Mini-batch size | $\{16, 32, 64, 128\}$ | B |
| Input sequence length | $\{1, 7, 14\}$ days | T_in |
| Optimizer | Fixed | Adam |
| Loss function | Fixed | MSE |
| Maximum epochs | 100 | E |
| Early-stopping patience | Fixed | epochs |
| Weight initialization | Fixed | Glorot uniform |
| Output layer | Fixed | Fully connected, 1unit |

### *3.3. Harris Hawks Optimization (HHO)*

The working principle of the HHO algorithm is based on simulating the collective hunting behavior of Harris hawks in nature through an integrated mathematical system that goes through successive and overlapping stages. The algorithm begins by creating a set of random solutions that represent the falcons' locations in the search space, then the prey (the best solution) is determined, expressed by X rabbit, which is the solution that all falcons seek to approach and surround through successive iterations [45]. The time to change the setting and the action are determined according to two main stages, and the transition between them is controlled by the energy factor. $T$ denotes the maximum number of iterations, and $E_0$ is the initial escaping energy of the prey, which is randomly generated within the interval $(-1, 1)$. The HHO operations are divided into:

- Exploration Phase: This includes light siege, heavy siege, and a surprise attack strategy based on a random coefficient value $q$ [46]. This is according to the following equation:

$$X(t+1) = \begin{cases} X_{\text{rand}}(t) - r_1 \left| X_{\text{rand}}(t) - 2r_2 X(t) \right| & q \geq 0.5 \\ \left( X_{\text{rabbit}}(t) - X_m(t) \right) - r_3 (LB + r_4 \left( UB - LB \right)) & q < 0.5 \end{cases} \tag{16}$$

$$X_m(t) = \frac{1}{N} \sum_{i=1}^{N} X_i(t) \tag{17}$$

where the prey is searched within the search space bounded by $[LB, UB]$. Here, $X$ represents the current position of a Harris hawk, $X_{\text{rabbit}}$ denotes the position of the prey (i.e., the current best or optimal solution), $X_{\text{rand}}$ is the position of a randomly selected Harris hawk, and $X_m$ is the average position of the Harris hawk population. The parameters $r_1$, $r_2$, $r_3$, $r_4$, and $q$ are random numbers uniformly distributed in the interval $[0, 1]$. The mathematical expression of $X_m$ is given at Equation (17).

- Exploitation Phase: This stage is divided into attack patterns determined based on the value of escaping energy $|E|$ and the random coefficient $r$ [47], considering the following strategies:

1. Strategy **A**: The soft attack: This pattern is activated when $r \geq 0.5$ and $|E| \geq 0.5$, as the falcons surround their prey with flexible movements according to:

$$X(t+1) = \Delta X(t) - E \left| J \cdot X_{\text{rabbit}}(t) - X(t) \right| \tag{18}$$

$$\Delta X(t) = X_{\text{rabbit}}(t) - X(t) \tag{19}$$

where $\Delta X(t)$ represents the difference between the position of the Harris hawk and the target (prey), and $J$ is a random number uniformly distributed in the interval $[0, 2]$.

2. Strategy **B**: The hard besiege. This activates when $r \geq 0.5$ and $E < 0.5$, where the hawks directly and decisively close the noose on their prey. In other words, this point represents one of the best solutions, as follows:

$$X(t+1) = X_{\text{rabbit}}(t) - E \left| \Delta X(t) \right| \tag{20}$$

3. Strategy **C**: Nice siege with fast and progressive dives. This strategy is based on the following:

$$X_{t+1} = \begin{cases} Y : X_{\text{rand},t} - E \left| X_{\text{rand},t} - X_t \right|, & F(Y) < F(X_t), \\ Z : Y + S \times \text{LF}(D), & F(Z) < F(X_t). \end{cases} \tag{21}$$

where $D$ denotes the problem dimension, and $S$ represents a randomly generated $D$-dimensional row vector.

4. Strategy **D**: A swift and indirect rush to the fierce siege. When $|E| < 0.5$ and $r < 0.5$, the prey lacks sufficient escape energy and becomes trapped, causing the Harris hawk to adopt a more aggressive encircling strategy to reduce the average distance between itself and the prey. The corresponding position update mechanism is expressed as follows:

$$X_{t+1} = \begin{cases} Y : X_{\text{rand},t} - E \left| J X_{\text{rand},t} - X_{m,t} \right|, & F(Y) < F(X_t), \\ Z : Y + S \times \text{LF}(D), & F(Z) < F(X_t). \end{cases} \tag{22}$$

Figure 6 illustrates how the HHO algorithm is employed to automatically tune a set of key parameters for the LSTM, with the aim of determining the optimal configuration that significantly enhances the performance of the model [48]. These key parameters include the learning rate, the number of hidden units, the batch size, the interruption rate to mitigate over-alignment, and the number of LSTM layers that make up the deep learning architecture.

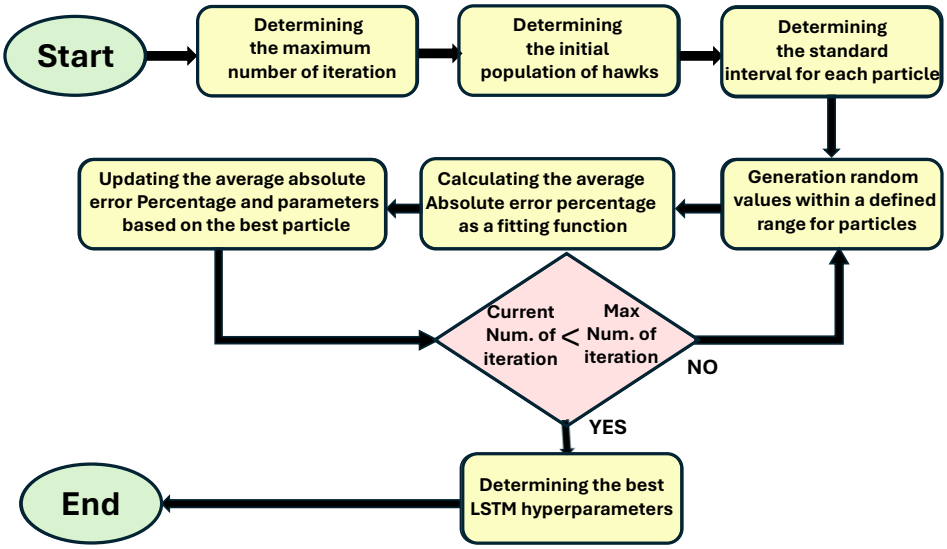



**Figure 6.** The HHO-LSTM control logic and decision-making flowchart.

Figure 7 is interpreted as follows:

1. Initialization: An initial "population" consisting of N randomly generated candidate operating policies is created. Each candidate policy is simply a vector of discharge values:
$$\mathbf{X}_i = [R_{i,1}, R_{i,2}, \ldots, R_{i,t}] \quad (23)$$
representing the volume of water released during each half hour of the study period. Each policy must fall within permissible limits (for discharge and storage), and input data (inflow, demand, elevation-storage curve, efficiency, and turbine capacity) are loaded. The iteration counter is set to iter = 0.
2. Reservoir Simulation and Fitness Evaluation: Each candidate policy is applied to the reservoir on a half-hour basis using the water balance equation, and energy production is calculated using the formula:
$$P_t = \frac{\eta \rho g Q_t H_t}{10^6} \quad (24)$$
where $P_t$ is hydropower output at time $t$, $\eta$ is overall turbine-generator efficiency, $\rho$ is water density (kg/m³), $g$ is gravitational acceleration (m/s²), $Q_t$ is turbine discharge at time $t$ (m³/s), and $H_t$ is the effective hydraulic head at time $t$ (m). A single fitness value (F) is assigned to the policy using a weighted multi-objective function that balances energy revenue against water supply deficits, water spillage, and any constraint violations. The policy with the lowest F value becomes $X_{(best)}$: the best solution currently known.
3. Decaying Energy Factor (Ĕ): A control parameter starts at a value from −2 to 2 and moves toward zero as iterations progress:
$$\check{E} = 2\,\check{E}_0\left(1 - \frac{iter}{iter_{max}}\right) \quad (25)$$

This factor determines the breadth or narrowness of the search range.

4. Search Phase Selection: For each candidate solution, the value of $|\check{E}|$ (along with a random number q or r) is considered to select the search mode:
($|\check{E}| \geq 1$) Exploration: Constructing entirely new and radically different release schedules to scan the full probability space of rule curves and avoid getting trapped in local optima.
($|\check{E}| < 1$) Exploitation: Staying close to the best solution (X-best) and making fine adjustments to it.
5. Policy Update Strategies: When the system is in exploitation mode, one of four operators modifies the release schedule; the operator is selected based on the values of $|\check{E}|$ and r:
Soft besiege: Minor adjustments to monthly release quantities around the best solution (X-best).
Hard besiege: Strongly pulling the schedule toward the best solution (X-best).
Soft besiege with dives: Using Lévy flight that maintains a large, non-repetitive random jump to escape a poor policy associated with the dry season.
Hard besiege with dives: A leap based on the average of the group (population) policies; it represents the highest degree of concentration. A new trial policy is retained only if its fitness value (F) is superior.
6. Feasibility Check and Repair: The modified schedules are reviewed against actual physical project constraints: turbine discharge limits, storage and flood control capacity, minimum environmental flow, and guaranteed energy requirements. Infeasible schedules are processed (modified/trimmed) or penalized; subsequently, they are re-evaluated, and the best solution (X-best) is updated.
7. Termination Condition: Check whether the algorithm has reached the maximum number of repetitions, or whether the improvement in the efficiency or fitness index has stalled.
8. Optimal Reservoir Operating Policy: Outputs the optimal policy (X*), which is the optimized half-hour release schedule and its corresponding storage trajectory, along with the resulting performance indicators annual energy and plant load factor, as well as reliability, resilience, and spill volumes.

Following the order, the data are split into 70% training, 15% validation and 15% testing. As illustrated in Table 5, it becomes clear that the HHO-LSTM model tops the list of similar models with the best overall performance, recording the lowest root mean square error (RMSE) of 0.0102, the lowest mean absolute error (MAE) of 0.0085, and the highest coefficient of determination ($R^2$) of 0.9831, which means that the model explains approximately 98.46% of the total variance in the data.

Moreover, a sensitivity analysis was conducted to evaluate the robustness of the proposed HHO-LSTM model against variations in input variables and hyperparameters. The proposed HHO-LSTM model outperformed the GA-LSTM model across all evaluation metrics. Specifically, the RMSE decreased from 0.0184 to 0.0102, representing an improvement of 44.57%, while the MAE was reduced from 0.0157 to 0.0085, corresponding to an improvement of 45.86%. Furthermore, the coefficient of determination $R^2$ increased from 0.905 to 0.9831, yielding an 8.63% improvement. These results demonstrate that the HHO algorithm provides more effective hyperparameter optimization than the GA algorithm, resulting in enhanced prediction accuracy and model generalization; these results are illustrated in Table 6.

**Table 5.** Performance comparison of models on test dataset.

| Model | RMSE | MAE | $R^2$ |
|---|---|---|---|
| RNN | 0.4563 | 0.0382 | 0.790 |
| LSTM | 0.2517 | 0.0205 | 0.830 |
| GA-LSTM [41] | 0.0184 | 0.0157 | 0.905 |
| WOA-LSTM [49] | 0.0157 | 0.0124 | 0.960 |
| HHO-LSTM | 0.0102 | 0.0085 | 0.9831 |

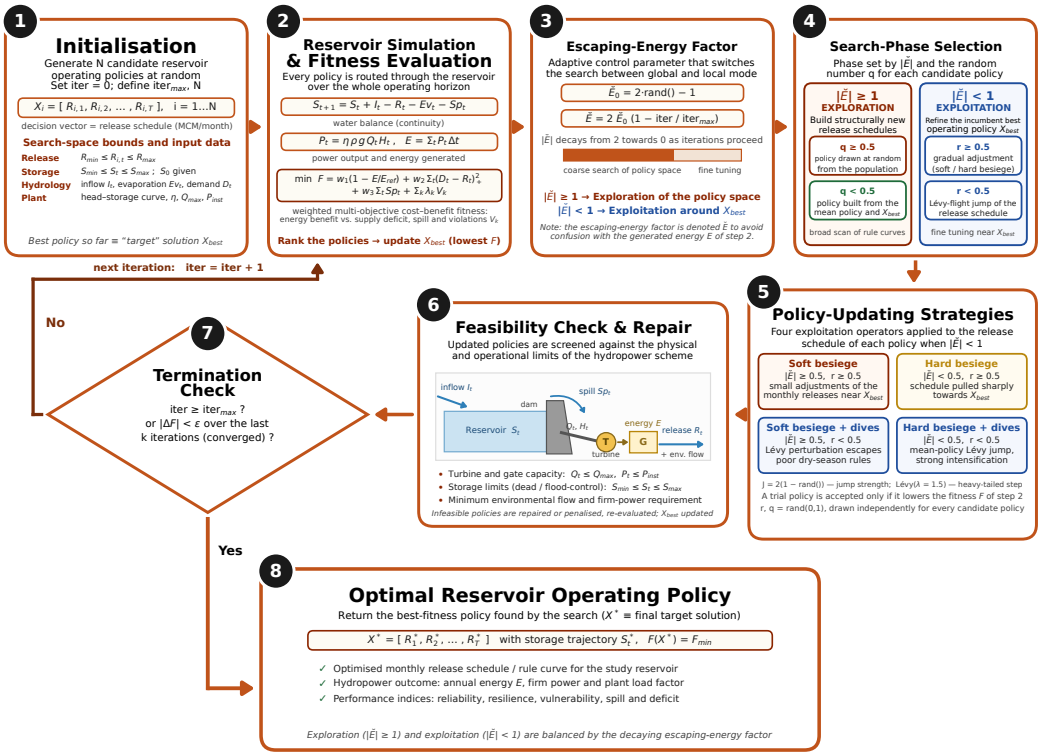



**Figure 7.** Harris Hawks Optimization steps.

**Table 6.** Improvement comparison among GA-LSTM, WOA-LSTM, and HHO-LSTM models.

| Metric | GA-LSTM/WOA-LSTM | GA-LSTM/HHO-LSTM | WOA-LSTM/HHO-LSTM |
|---|---|---|---|
| RMSE | 14.67% | 44.57% | 35.03% |
| MAE | 21.02% | 45.86% | 31.45% |
| $R^2$ | 6.08% | 8.63% | 2.20% |

### *3.4. The IMOHHO-LSTM Simulation Model*

The optimization design is based on direct control of the opening rates of the dam gates; as shown in Table 3, there are six gates and 48 time periods, occurring every 30 min. The decision vector can be expressed as follows:

$$X = [G_{1,1}, G_{2,1}, \ldots, G_{6,48}] \tag{26}$$

where $G_{i,t}$ represents the opening ratio of gate $i$ at time $t$. Therefore, the number of decision variables is equal to:

$$n_{var} = N_g \times T = 6 \times 48 = 288 \tag{27}$$

all decision variables were limited to:

$$0 \leq G_{i,t} \leq 100 \tag{28}$$

within the algorithm, and solutions are stored in their natural form that considers ($0 \leq X \leq 1$), then converted into percentages during evaluation as follows:

$$G = 100X \tag{29}$$

each solution generated by IMOHHO-LSTM is sent directly to the simulation model. The model consists of four parts: gate discharge model, water reservoir model, head model, and turbine model. The discharge rate was calculated using the following:

$$X \rightarrow GateDischarge \rightarrow ReservoirSimulation \rightarrow ObjectiveFunction \tag{30}$$

the discharge rate from each gate was calculated using the following:

$$Q_i = C_d A_i \sqrt{2gH} \tag{31}$$

with the area of a single gate opening represented as follows:

$$A_i = W_g H_g O_i \tag{32}$$

where $O_i$ is:

$$O_i = \frac{G_i}{100}$$

updating the reserve storage in the dam reservoir relies on the following water balance equation:

$$S_{t+1} = S_t + (Q_{in} - Q_{release})\Delta t \tag{33}$$

with the following application of restrictions to it:

$$S_{min} \leq S_t \leq S_{max} \tag{34}$$

additionally, to connect the hydraulic net head to the reservoir equation, the researchers considered:

$$H_t = f(S) \tag{35}$$

where $H_t$ is defined as follows:

$$22 \text{ m} \leq Ht \geq 46 \text{ m} \tag{36}$$

to calculate the electrical energy generated from the utilized discharge, we considered the 410 following discharge volumes used for generation:

$$Q_T = \min(Q_{release}, Q_{T,max}) \tag{37}$$

the generated power is defined as follows:

$$P = \eta \rho g Q_T H_t \tag{38}$$

the $P_{MW}$ means Power in Megawatts and is represented as follows:

$$P_{MW} = \frac{P}{10^6} \tag{39}$$

with the following limit:

$$P \leq 660MW \tag{40}$$

we identified five objectives, and we will show how they were achieved in this paper.

- Objective 1: Maximizing the electrical energy produced from the dam, as follows:

$$f_1 = -\sum_{t=1}^{T} P_t \Delta t \tag{41}$$

The "−" in Equation (41) means that energy is leaving the water storage. Therefore, the change in the energy of the dam reservoir is negative. If we want to calculate the energy directly, we can use the following equation:

$$E_{\text{generated}} = \sum_{t=1}^{T} P_t \Delta t \tag{42}$$

- Objective 2: Reducing the storage change in the dam lake below the required level, as follows:

$$f_2 = \frac{1}{T} \sum |S_t - S_{target}| \tag{43}$$

- Objective 3: Minimizing excess water discharge as much as possible, as follows:

$$f_3 = \sum Spill_t \tag{44}$$

- Objective 4: Controlling gate movement to regulate the volume of water consumed and the electrical power generated by the turbines, as follows:

$$f_4 = \sum |G_t - G_{t-1}| \tag{45}$$

- Objective 5: Reducing the deficit in power generated by the dam, as follows:

$$f_5 = \frac{\sum (P_{max} - P_t)}{P_{max} T} \tag{46}$$

Modifications Introduced in IMOHHO

The original HHO [48] is a single-objective optimizer with a single global best. Three modifications were required to apply it to the present problem, and they are stated separately here as shown in Table 7 so that each can be assessed individually.

External Pareto archive with crowding distance pruning: The single "rabbit" of the original algorithm is replaced by an external archive $\mathcal{A}$ of mutually non-dominated schedules. After every iteration the archive is updated by the dominance test of Equation (60), and when $|\mathcal{A}|$ exceeds the capacity $N_{\mathcal{A}}$, members are removed in increasing order of crowding distance

$$d_k = \sum_{m=1}^{M} \frac{f_m^{(k+1)} - f_m^{(k-1)}}{f_m^{\max} - f_m^{\min}}, \tag{47}$$

where $M = 5$ is the number of objectives and the superscripts denote the neighbors of solution $k$ in the sorted order of objective $m$. Boundary solutions are assigned an infinite distance and are therefore retained.

Probabilistic leader selection from sparse archive regions: At each iteration the leader $X_{\text{leader}}$ that replaces $X_{\text{rabbit}}$ in Equations (18) and (20) is drawn from the archive with probability proportional to crowding distance,

$$\Pr(X_{\text{leader}} = X_k) = \frac{d_k}{\sum_{l \in \mathcal{A}} d_l}, \tag{48}$$

so that the search is biased towards under-represented regions of the front. Uniform selection from the archive, used as the ablation control, concentrates the population in the densest region.

Constraint-aware repair operator: Rather than penalizing infeasible schedules in the objective function, candidate schedules are projected onto the feasible set before evaluation. Gate openings are clipped to $[0, 100]$; successive openings are limited by the physical gate movement rate,

$$|G_{i,t} - G_{i,t-1}| \leq \Delta G_{\max}, \tag{49}$$

with $\Delta G_{\max} = dG\%$ per 30 min step; and if the simulated storage trajectory violates $S_{\min} \leq S_t \leq S_{\max}$, the openings from the first violating step onward are scaled by the factor that restores the bound. Because repair acts before evaluation, every schedule in the archive is operationally implementable, which is not guaranteed by a penalty formulation.

**Table 7.** Summary of the proposed IMOHHO–LSTM gate scheduling procedure.

| Step | Operation | Description |
|---|---|---|
| Input | LSTM inflow forecast | Provide the predicted inflow sequence $\hat{Q}_{\text{in},1:T}$, population size $N$, archive capacity $N_{\mathcal{A}}$, and maximum iterations $T_{\max}$. |
| 1 | Population initialization | Initialize $N$ candidate gate schedules $X_i \sim \mathcal{U}(0, 100)^{N_g \times T}$. |
| 2 | Constraint handling (M3) | Apply $\textsc{Repair}(X_i)$ to enforce the applicable gate-operation constraints. |
| 3 | Objective evaluation | Evaluate $\mathbf{F}(X_i)$ using hydraulic simulation and initialize the Pareto archive $\mathcal{A}$ with non-dominated candidates. |
| 4 | Escape energy calculation | Generate $E_0 \sim \mathcal{U}(-1, 1)$ and calculate $E = 2E_0\left(1 - \frac{t}{T_{\max}}\right)$. |
| 5 | Leader selection (M2) | Select $X_{\text{leader}}$ from $\mathcal{A}$ according to Equation (48). |
| 6 | Exploration and exploitation | If $\lvert E \rvert \geq 1$, apply the exploration rule in Equation (16). Otherwise, apply the exploitation rule selected according to $\lvert E \rvert$ and $r$ using Equation (18). |
| 7 | Schedule repair and evaluation | Repair each updated schedule and evaluate its objective vector using hydraulic simulation. |
| 8 | Archive update | Insert non-dominated candidate schedules into $\mathcal{A}$ and remove dominated solutions. |
| 9 | Archive maintenance (M1) | If $\lvert \mathcal{A} \rvert > N_{\mathcal{A}}$, prune the archive using crowding distance, as defined in Equation (47). |
| Output | Pareto archive | Return $\mathcal{A}$ containing the retained non-dominated gate schedules. |

Algorithm initialization is defined as shown in Table 8 and follows:

$$X_i = VarMin + rand(VarMax - VarMin) \tag{50}$$

prey escape energy is calculated as follows:

$$E = 2E_0\left(1 - \frac{t}{T}\right) \tag{51}$$

the Falcon Exploration is calculated as follows:

$$X^{t+1} = X_{leader} - r|X_{leader} - 2rX| \tag{52}$$

exploitation is calculated as follows:

$$X^{t+1} = X_{leader} - E|X_{leader} - X| \tag{53}$$

lévy flight is defined as follows:

$$X^{t+1} = X^{t+1} + S \times LF(D) \tag{54}$$

we create a Pareto archive where each new solution undergoes a dominance test as follows:

$$X_a \prec X_b \tag{55}$$

the test is coming out well if:

$$f_i(X_a) \leq f_i(X_b) \tag{56}$$

at least one of our five goals is achieved if:

$$f_i(X_a) < f_i(X_b) \tag{57}$$

the final solution is selected after the optimization is completed, and the running schedule is sent to the simulation model to produce the final results (Table 9).

**Table 8.** Hyperparameter settings for the proposed IMOHHO algorithm.

| Parameter | Value | Description |
|---|---|---|
| Population size ($N$) | 100 | Number of candidate hawks in the swarm |
| Max iterations ($T_{\max}$) | 500 | Stopping criterion for the optimization loop |
| Archive size ($N_{\text{arc}}$) | 100 | Maximum number of non-dominated Pareto solutions |
| Decision dimension ($D$) | 288 | 48 time intervals × 6 spillway gates |
| Search space bounds | $[0.0, 1.0]$ | Normalized gate fractional opening |
| Lévy flight parameter ($\beta$) | 1.5 | Power-law index for heavy-tailed distribution |
| Leader selection pressure | 2.0 | Roulette-wheel selection bias towards sparse regions |
| Independent runs | 30 | Repetitions for statistical significance testing |

**Table 9.** Distinction between the original HHO, baseline multi-objective HHO, and the proposed IMOHHO framework.

| Feature | Original HHO | Baseline Multi-Objective HHO | Proposed IMOHHO |
|---|---|---|---|
| Optimization type | Single-objective | Multi-objective | Multi-objective dam gate scheduling |
| Fitness evaluation | Scalar fitness value | Pareto dominance | Pareto dominance |
| Output | One best solution | Set of non-dominated solutions | Set of feasible Pareto-optimal gate schedules |
| Elite solution storage | Best rabbit/prey | External Pareto archive | External Pareto archive |
| Leader selection | Single best rabbit | Archive-based or random archive leader | Select Leader strategy |
| Search mechanism | HHO exploration and exploitation | HHO exploration and exploitation | HHO exploration and exploitation |

**Table 9.** *Cont.*

| Feature | Original HHO | Baseline Multi-Objective HHO | Proposed IMOHHO |
|---|---|---|---|
| Escaping energy mechanism | Included | Included | Included; inherited from original HHO |
| Lévy-flight perturbation | Included in HHO variants | May be included | Included; inherited from original HHO |
| Decision representation | General continuous variables | General multi-objective variables | 288-dimensional gate-operation schedule |
| Decision variable bounds | Problem-dependent | Problem-dependent | Normalized within $[0, 1]$ |
| Scheduling horizon | Not applicable | Problem-dependent | 48 intervals $\times$ 30 min $=$ 24 h |
| Dam operation constraints | Not applicable | Problem-dependent | Storage, release, turbine flow, gate opening, and gate movement constraints |
| Main contribution | Original HHO | Pareto-based HHO extension | Integrated Pareto-based HHO scheduling framework for Haditha Dam |

## 4. Results and Discussion

This section aims to analyze the performance of the proposed intelligent control framework based on the improved IMOHHO-LSTM algorithm for a Haditha Dam operation. The performance of the algorithm was evaluated using a developed hydraulic simulation model linking gate operation, storage and discharge, hydraulic head and hydropower generation. The evaluation focused on five key operational objectives: maximizing power generation, maintaining storage near the target level, minimizing unused discharge, minimizing fluctuations in gate openings, and minimizing the power generation deficit. The system optimized the operational schedule over 48 time steps, where each step represented a 30 min interval covering a full day of operation. A set of solutions was generated using the algorithm and subsequently evaluated via the simulation model. Only the undominated solutions were then kept in the Pareto archive. The final results showed that the IMOHHO-LSTM algorithm was able to reach stable solutions that achieved a clear balance between all conflicting objectives, which was directly reflected in the stability of the storage level and the increase in average production capacity while maintaining the safe operating limits of the dam.

### *4.1. Dam Gate Operation Analysis*

Figure 8 shows the opening rates of the six gates determined by the IMOHHO-LSTM algorithm during the optimal operation period. These gate opening rates represents one of the most important outputs of the optimization process, because it directly reflects how the algorithm makes gate control decisions to balance power generation and maintain water reservoir stability.

The figure shows that the algorithm did not depend on all gates being opened equally. Instead, it distributed opening percentages irregularly across the six gates. This indicates that the optimization process aimed not just to increase discharge, but to determine the optimal discharge distribution that maximized operational efficiency. The results showed that some gates operated with relatively high opening rates, while others remained with low or medium opening rates. This is because the simulation model took into account all operational constraints, including: total discharge limits, storage level, turbine design capacity, and gate operation. This behavior reflects the ability of the algorithm to avoid traditional solutions that rely on fully opening all gates that often lead to reservoir depletion

without achieving an appreciable increase in power production, especially when the maximum capacity of the turbine is predetermined. It was also noted that the changes between successive time periods were relatively gradual, which indicates the success of the fourth goal regarding controlling the movement of the gate. This result is operationally important, because it reduces mechanical stress on the gate system and extends the operational life of the equipment. It can be inferred from this figure that the IMOHHO-LSTM algorithm succeeded in achieving an intelligent distribution of discharge between gates, where the operation of each gate depended on the instantaneous hydraulic conditions rather than fixed operating rules. This enhanced system efficiency and increased operational flexibility in response to fluctuations in flow, and it can be said that one objective was achieved.

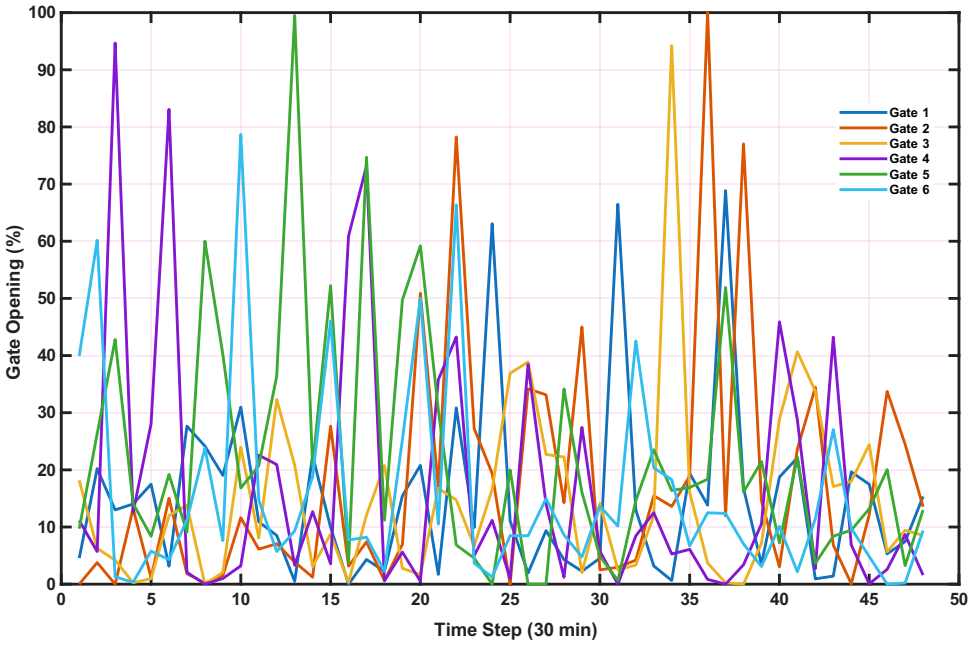



**Figure 8.** Haditha Dam gate opening schedule curves.

### *4.2. Dam Reservoir Storage Level*

The storage level in the dam's reservoir is a key indicator for evaluating operational efficiency, because it directly reflects the ability of the control system to achieve a balance between inflows and outflows while maintaining the water reserves necessary to meet future demands. In multi-purpose dams, operational objectives extend beyond maximizing hydropower generation to include maintaining storage stability within safe operating limits and minimizing the risk of flooding or reservoir depletion during periods of low water flow. A target storage value has been adopted here, amounting to:

$$S_{target} = 2200\,\mathrm{Mm}^3$$

This objective is incorporated into a multi-objective optimization function, where the IMOHHO-LSTM algorithm seeks to minimize the average deviation from this level throughout the run. Figure 9 shows the temporal variation in storage volume inside the Haditha Dam reservoir during the optimal operating cycle derived from the proposed algorithm.

Figure 9 shows that the storage level remained very close to the target value throughout the runtime, with the storage size ranging between 2199.20 $\mathrm{Mm}^3$ and 2206.74 $\mathrm{Mm}^3$. In other words, the extent of the total change did not exceed approximately 7.54 $\mathrm{Mm}^3$. This is a very small change compared to the operating capacity of the water reservoir, suggesting that the control system was able to maintain a near-stable state of the water reservoir despite the constant fluctuations in internal flow decisions and gate operations. It is also noted that the

storage curve does not show any sharp fluctuations or sudden declines; instead, it follows a smooth, gradual path around the target storage level.

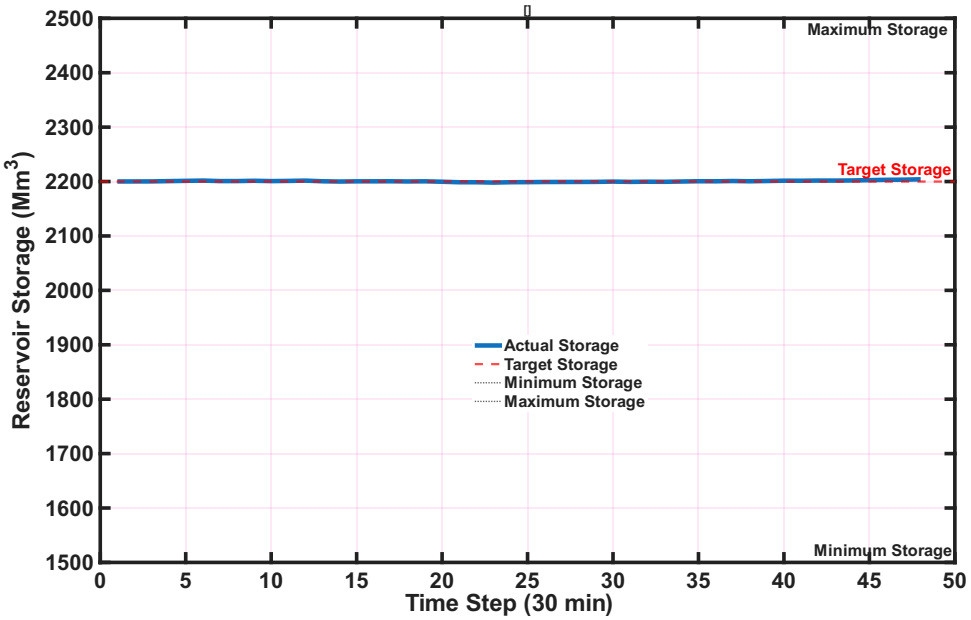



**Figure 9.** Haditha Dam reservoir storage variation.

This behavior reflects the success of the IMOHHO-LSTM algorithm in achieving the main optimization goal: minimizing the deviation in storage levels from the reference point while maintaining continuous hydropower generation. The horizontal line representing the target storage level serves as the main reference to evaluate the performance of the algorithm. The figure shows that most storage values remain within a narrow range around this level. Operationally, maintaining storage levels near the target range offers several important advantages, including ensuring sufficient water reserves to handle future fluctuations in water flow, reducing the potential for low hydraulic head affecting energy production, and reducing the risk of exceeding upper storage limits during flood periods.

The results also show that the hydraulic simulation model, when combined with the IMOHHO-LSTM algorithm, achieved a balanced dynamic response between inflow and outlet water flow. Gate openings are continuously adjusted to maintain storage stability without requiring major operational changes. This confirms that the algorithm not only seeks to maximize energy production but also takes into account all operational constraints associated with reservoir management. These results are consistent with recent trends in multi-purpose water reservoir operation, which emphasize that optimal operation is not just about maximizing energy production, but also about achieving a sustainable balance between power generation, maintaining storage, and mitigating operational risks. This balance represents a major advantage of multi-objective optimization algorithms over traditional operating methods, which rely on fixed rules and fail to take into account temporal changes or fluctuating operating conditions. Overall, Figure 9 demonstrates that the proposed algorithm successfully maintained a high level of reservoir stability, keeping storage levels close to the reference value throughout the operational period. This provides a solid foundation for sustainable hydroelectric power generation and enhances the operational reliability of the Haditha Dam under varying operating conditions. Thus, it can be concluded that the second objective has also been achieved.

### *4.3. Hydroelectric Power Generation*

Maximizing hydropower generation is the primary goal in most multi-purpose dam operating systems, given their great economic and operational importance. However, achieving peak power production must not come at the expense of water reservoir stability or operational safety. Therefore, power generation is integrated into a multi-objective optimization framework that enables the algorithm to balance all operational requirements. Figure 10 shows the variation over time in the electrical energy generated by Haditha Dam power station during the period of optimal operation, as well as the design capacity of the station and the average total power production. That power output remains high throughout most of the operating period, with limited fluctuations resulting from normal variations in vacuum and hydraulic head. The average power output is:

$$P = 434.76\,\text{MW}$$

and the maximum power reached is:

$$P = 660\,\text{MW}$$

it is equivalent to the maximum design capacity of a hydropower plant. And the total energy generated during the operating cycle in one day is:

$$E_{total} = 10{,}434.14\,\text{MWh}$$

this is also a high value, reflecting the algorithm's success in making effective use of available water resources. To give a clearer picture of the plant's utilization level, the capacity utilization factor can be calculated as follows:

$$CUF = \frac{\overline{P}}{P_{rated}} \times 100 \tag{58}$$

by substitution, it is:

$$CUF = \frac{434.76}{660} \times 100 = 65.872\% \tag{59}$$

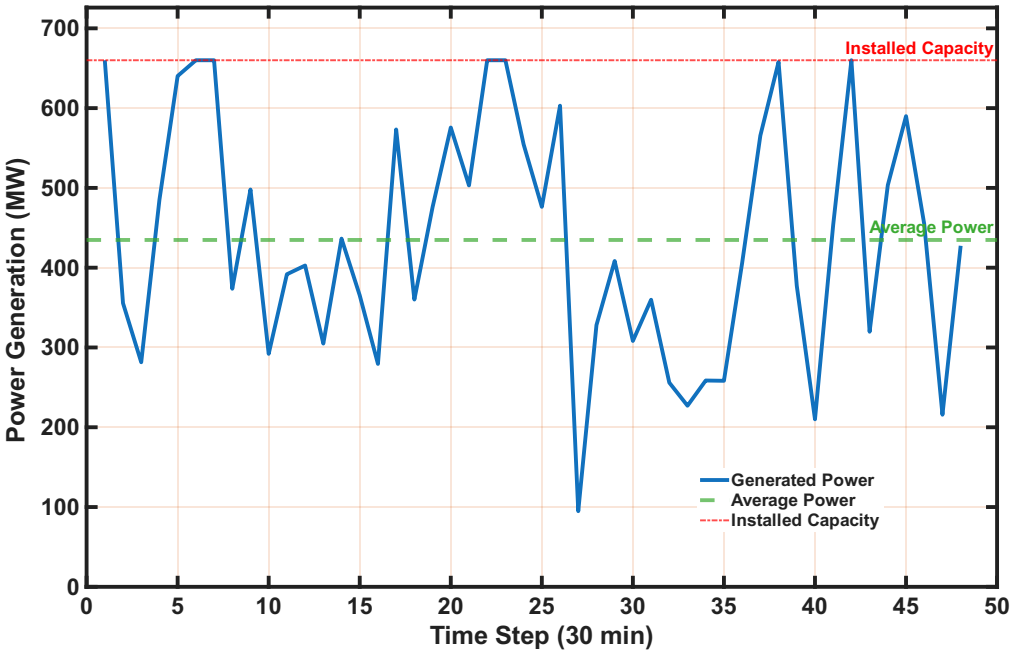



**Figure 10.** Haditha Dam hydropower curve.

Figure 10 indicates that the power plant operated at an average of about 66% of its design capacity throughout the operation, a high rate compared to traditional operating systems that often experience a drop in output due to static operation or not responding quickly to water flow fluctuations. It was also observed that the energy output curve did not remain at the maximum value of 660 MW throughout the period; this behavior is a positive indicator, as it shows that the algorithm was not intended to continuously maintain the plant at maximum capacity, and adhered to drainage restrictions while avoiding unnecessary water drainage. If the sole goal was to maximize capacity, the turbine would have operated at maximum discharge throughout the operating life; this would have resulted in a rapid reduction in storage volume and a decrease in hydraulic head, reducing performance in the long term.

It is also worth noting that the average power output closely corresponds to the design capacity of the plant. This demonstrates the ability of the IMOHHO-LSTM algorithm to ensure stable turbine operation while minimizing large fluctuations in electricity generation in response to variable load requirements. Static power output is a vital factor in electrical power systems, as it enhances the reliability of supply and reduces the need for backup generation sources. This performance is directly related to the algorithm's ability to intelligently control gate openings, as the aperture ratios are dynamically adjusted to maintain an appropriate discharge rate, ensuring continuous power generation without exceeding the turbine operating limits. This resulted in a clear balance between inlet water flow, storage levels, and power output, confirming the successful integration of the hydraulic simulation model with the multi-objective optimization algorithm.

Overall, Figure 10 shows that the proposed framework achieved high operational performance; the average power generated was close to the design capability of the plant while maintaining operational stability throughout the simulation period. These results confirm that the IMOHHO-LSTM algorithm provides an efficient mechanism to maximize hydropower generation without exceeding dam operation constraints, making it suitable for application in multi-purpose smart dam management systems. So, we can confidently say that the third goal has been achieved.

### *4.4. Pareto Front Analysis*

The Pareto front is a key tool in multi-objective optimization problems, as it represents the set of non-dominated solutions that achieve the best possible balance among conflicting objectives without prioritizing one objective absolutely at the expense of others. In this study, the IMOHHO-LSTM algorithm employs the concept of Pareto dominance to evaluate candidate solutions, retaining only those that achieve the best collective performance regarding the five objective functions defined in the optimization model. Figure 11 shows the Pareto front resulting from the optimization process, explaining the relationship between the non-dominant solutions obtained after completing all iterations of the algorithms.

Figure 11 and Table 10 show that the algorithm successfully generated a variety of non-dominant solutions rather than converging on a single solution, which is a key feature of multi-objective optimization algorithms. The distribution of points along the Pareto front indicates that each point represents a distinct operating policy, achieving a specific balance between energy production, storage conservation, minimizing unused discharge, minimizing gate opening fluctuations, and minimizing capacity deficits. Solutions on the Pareto front are known to satisfy the conditions described below. However, the best solution

based on the choice of algorithm is the tenth point if the electrical power is required, the details of which are given in Table 10.

$$X_a \prec X_b \iff \begin{cases} f_i(X_a) \leq f_i(X_b), & \forall i \\ \exists j : f_j(X_a) < f_j(X_b) \end{cases} \tag{60}$$

where $\prec$ is the Dominance Operator Read indicating dominance. $X_a \prec X_b$ means $X_a$ is a better solution than $X_b$ under Pareto criteria.

$X_a$, $X_b$ are two candidate solutions being compared, each representing a set of decision variables proposed to solve the optimization problem.
$f_i()$ is the objective function with the $i$-th criterion to be minimized, evaluated for a given solution.
$i$ is the Objective Index running over all objectives $i = 1, 2, \ldots, n$.
$j$ is the Strict Improvement Index for which $X_a$ is strictly better than $X_b$.
$\forall\, i$ means that the condition must hold for every objective without exception.

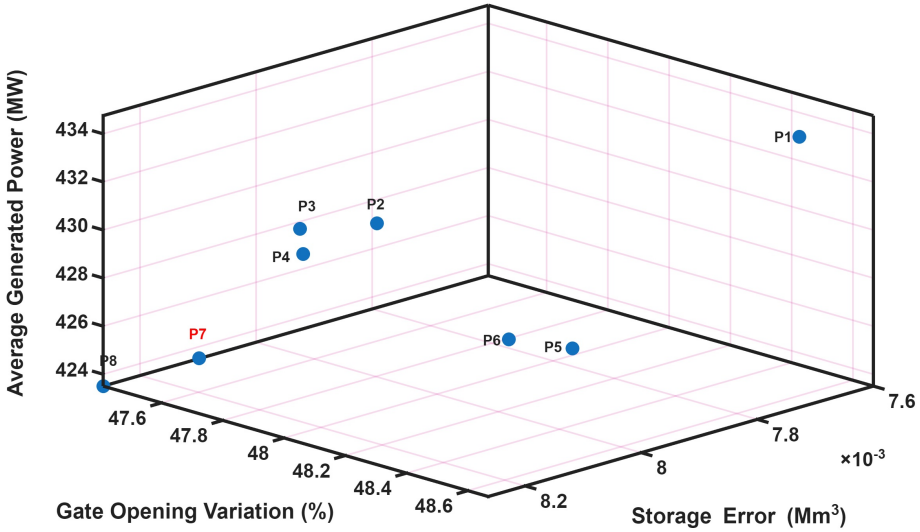



**Figure 11.** 3D Pareto front for the 22 power generation objective.

**Table 10.** Best solution for Haditha Dam by high electricity production.

| Parameter | Value |
|---|---|
| Selected Pareto Solution | P7 |
| Hydropower Generation | 10,434.14 MWh |
| Average Generated Power | 434.76 MW |
| Installed Capacity | 660.00 MW |
| Maximum Generated Power | 660.00 MW |
| Maximum Release | 942.54 $m^3/s$ |
| Minimum Reservoir Storage | 2199.62 $Mm^3$ |
| Maximum Reservoir Storage | 2213.12 $Mm^3$ |

Figure 11 illustrates that solutions at one end of the Pareto front achieve higher levels of energy production but are accompanied by increases in other performance indicators such as discharge or storage drift, while solutions at the opposite end provide greater water reservoir stability at the expense of a slight decrease in energy production. This behavior embodies the concept of trade-off, which forms the theoretical basis of multi-objective optimization, since it is impossible to optimize all objectives simultaneously to their best

possible values. Upon completion of the optimization process, one of the non-dominant solutions from the Pareto archive was selected as the final operating policy. This choice was based on achieving the solution for the best balance of all performance indicators, rather than achieving a single goal to the maximum. The simulation results showed that the chosen solution achieved the results outlined below.

In other words, any attempt to improve one goal necessarily deteriorates another. Therefore, there is no single solution that can be considered the absolute best. Instead, there are a range of optimal solutions that strike different balances between conflicting goals. It can be seen from Figure 12 that solution *P*9 aims to maximize the volume of outflow water from the dam while maintaining the reservoir level, without considering electricity generation, and Table 11 shows this clearly. The other points represent other solutions. This indicates that the algorithm maintains the diversity of solutions during the search process. Maintaining diversity is a fundamental requirement in multi-objective optimization algorithms, because it provides the decision-maker with a wider range of operational alternatives that can be chosen based on dam management priorities. This performance is attributed to the use of the Pareto archive. After each iteration, the algorithm removes the dominant solutions and keeps only the non-dominated solutions. The crowding distance criterion is then used to maintain the diffusion of solutions along the interface and prevent them from clustering in a particular region of the solution space. As a result, IMOHHO-LSTM achieves a suitable balance between exploration and exploitation, thus enhancing the quality of the final interface.

**Table 11.** Final Haditha Dam results for maximum release.

| Parameter | Value |
|---|---|
| Selected Pareto Solution | P9 |
| Hydropower Generation | 8796.96 MWh |
| Average Generated Power | 366.54 MW |
| Maximum Generated Power | 660.00 MW |
| Installed Capacity | 660.00 MW |
| Maximum Release | 1013.71 $m^3/s$ |
| Minimum Reservoir Storage | 2199.72 $Mm^3$ |
| Maximum Reservoir Storage | 2215.39 $Mm^3$ |

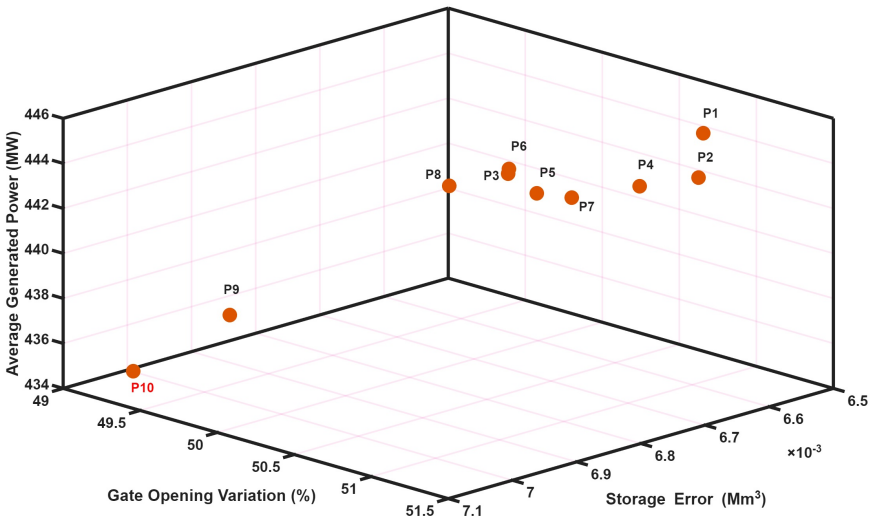



**Figure 12.** 3D Pareto front for the maximum-release objective.

The results in Table 12 and Figure 13 indicate that the optimal solution was not just the solution that achieved the fixed Head Net, but rather the solution that provided the best operational balance between all objectives. This reflects the effectiveness of the IMOHHO-LSTM algorithm in addressing multi-objective engineering problems with complex operational constraints. In practice, the Pareto front provides decision-makers with great flexibility, allowing different solutions to be chosen based on operational conditions or management priorities. During periods of drought, an operator may choose a solution that maintains storage even at the cost of a slight reduction in energy production, while in times of abundant water, the choice may prioritize maximizing energy production while maintaining safe operating limits. Thus, the resulting front is not just a mathematical output of the algorithm, but a practical decision support tool for smart dam management.

Overall, the results confirm that the IMOHHO-LSTM algorithm successfully creates a Pareto front with good propagation and high quality, while maintaining diversity among non-dominated solutions. This confirms their ability to derive flexible and efficient operating policies for modern dams and demonstrates their suitability for improving multi-purpose reservoir operation in variable hydrological environments.

**Table 12.** Final Haditha Dam results.

| Parameter | Value |
|---|---|
| Selected Pareto Solution | P2 |
| Hydropower Generation | 5766.62 MWh |
| Average Generated Power | 240.28 MW |
| Maximum Generated Power | 432.88 MW |
| Installed Capacity | 660.00 MW |
| Maximum Release | 743.08 $m^3/s$ |
| Minimum Reservoir Storage | 2200.91 $Mm^3$ |
| Maximum Reservoir Storage | 2215.67 $Mm^3$ |

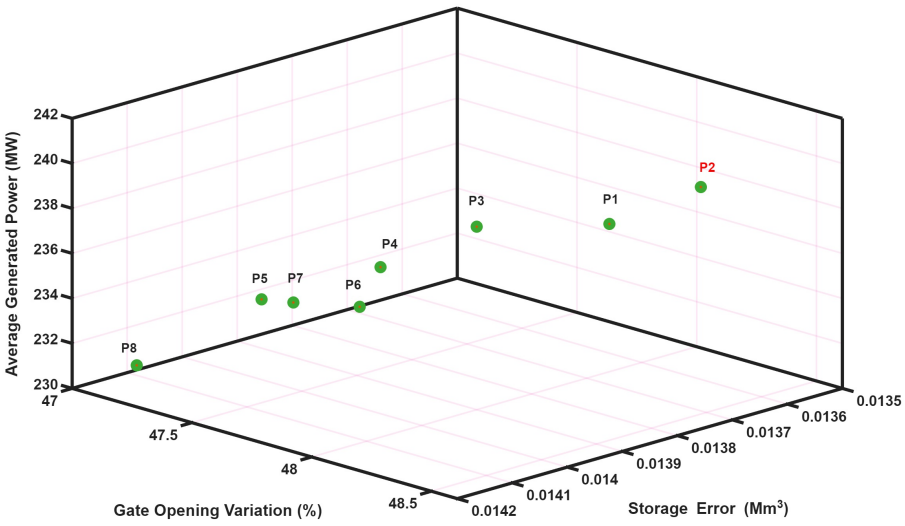



**Figure 13.** 3D Pareto front for the fixed Head Level objective.

## 5. Discussion of the Performance of the IMOHHO-LSTM Algorithm

The main goal of developing the framework proposed in this study was not simply to maximize hydropower generation, but to design an intelligent operating system capable of achieving a sustainable balance between a set of conflicting operational objectives governing the management of multi-purpose reservoirs. This problem is one of the most complex optimization challenges in water resource engineering, because all operational

variables within the water reservoir are interconnected by nonlinear relationships, and because any operational decision made at a given moment directly affects the system's performance in subsequent periods. Simulation results obtained using the multi-objective optimization IMOHHO-LSTM algorithm indicate that the proposed model successfully achieves an amazing balance between power generation, maintaining storage levels, and minimizing gate oscillations, while fully adhering to the operational constraints of Haditha Dam. The obtained results demonstrate the success of the optimization algorithm in taking advantage of the available hydraulic potential without compromising reservoir stability or exceeding the operational limits of the dam. Unlike many conventional operating methods, the proposed framework does not rely on fixed rule curves; instead, it dynamically updates gate opening decisions based on the actual state of the hydraulic system. This includes factors such as internal flow, storage level, net hydraulic head and power demand, along with operational limitations of turbines and gates. This integration of the hydraulic model and optimization algorithm results in more flexible operational decisions compared to methods based on human experience or fixed operating schedules. But one limitation of the current study is that IMOHHO has not been directly tested against adopted multi-objective optimization algorithms, such as NSGA-II or MOPSO, for the dam gate scheduling problem. The comparisons between GA, WOA, and HHO presented in Tables 3 and 4 relate to their impact on the accuracy of LSTM prediction and should not be interpreted as a comparative evaluation of multi-objective optimization performance. Accordingly, the current results show IMOHHO's performance under the conditions of the case study considered but do not prove its superiority over other multi-objective algorithms in terms of convergence or diversity of solutions. Future work will address this constraint through tight comparison using identical problem formulas and similar evaluation budgets, with frequency of operation and appropriate metrics of convergence, variety, and computational cost. Mathematically, the optimization process focused on minimizing the objective function vector can be defined as follows:

$$\mathbf{F}(X) = [f_1(X), f_2(X), f_3(X), f_4(X), f_5(X)] \tag{61}$$

where we can find the following functions:

- $f_1$ that maximize hydroelectric power generation.
- $f_2$ that minimize reservoir storage deviation from the target level.
- $f_3$ that minimize unutilized discharge (spill).
- $f_4$ that show the gate opening schedule.
- $f_5$ that minimize electric power capacity deficits.

This entails running a realistic mathematical model of the dam problem, since reservoir management in practical applications does not depend on a single goal. Rather, it seeks to achieve the best possible combination between a set of conflicting goals. These two goals are inherently opposed; increasing the turbine's discharge increases energy production but at the same time depletes the volume stored, so that maximum generation and maximum storage cannot be achieved at the same time. So the problem is multi-purpose, allowing not for a single example but for a set of non-dominant solutions (Pareto optimal), each representing a different trade-off between generation and storage. The present results confirm that integrating the hydraulic model with the IMOHHO-LSTM algorithm provides a flexible framework applicable to smart dam operation systems. The optimization process can be re-implemented in response to changing hydrological or operational conditions without the need to completely redesign the operating rules. This feature represents a major advantage of the proposed framework over traditional operational methods, which rely on fixed operating curves or manual decisions that rely heavily on operator experi-

ence. Table 13 below illustrates some current and future applications where the proposed algorithm can be utilized.

**Table 13.** Practical benefits of the proposed framework for Haditha Dam operations.

| Practical Application | Benefit |
| --- | --- |
| Storage Management | Maintaining storage volume stability and minimizing deviation from the target level. |
| Gate Operation | Dynamically distributing gate openings and limiting uncontrolled sudden fluctuations. |
| Energy Production | Enhancing water utilization efficiency and maintaining power output close to design capacity. |
| Decision Support | Providing a set of non-dominated operational alternatives based on operational requirements. |
| Smart Dams | Capability to integrate with SCADA systems and enable real-time monitoring. |
| Future Management | Scalability for the operation of multi-reservoir systems. |

## 6. Conclusions

This paper provided a comprehensive assessment of the performance of the proposed framework based on the IMOHHO-LSTM algorithm in optimizing the operation of Haditha Dam. This was achieved by analyzing gate operations, storage behavior, and hydropower generation, as well as examining non-dominant solutions resulting from the multi-objective optimization process. The Pareto front showed that the proposed model successfully generated a variety of non-dominant solutions, providing decision-makers with great flexibility in choosing appropriate operating policies based on hydrological conditions or power grid requirements. Furthermore, the comprehensive analysis revealed that integrating the hydraulic model with the IMOHHO-LSTM algorithm improved the management of the interrelationships between storage, hydraulic head, discharge and power generation, thus highlighting the efficiency of the framework in meeting multi-objective operational challenges. Finally, this paper showed that the proposed model holds promising practical potential for modern dam operations. It can be further developed to integrate with real-time monitoring systems and smart dam systems, or extended to manage multiple reservoir systems, thus serving as a suitable basis for the next developments, which addresses the general conclusions of the study, scientific contributions, and recommendations for future work.

**Author Contributions:** Conceptualization, A.S., Q.Z. and A.R.; methodology, A.S., B.A. and Q.Z.; software, A.S. and A.M.; validation, A.S., A.M. and O.A.; formal analysis, A.S. and Q.Z.; investigation, A.S.; resources, B.A., K.H. and Y.Q.; data curation, A.S. and A.M.; writing—original draft preparation, A.S.; writing—review and editing, A.S., B.A., M.K.M., Q.Z., O.A. and Y.Q.; visualization, A.S.; supervision, B.A. and A.R.; project administration, B.A., K.H. and M.K.M. All authors have read and agreed to the published version of the manuscript.

**Funding:** This research received no external funding.

**Data Availability Statement:** The complete source code for MATLAB that implements the proposed IMOHHO algorithm and simulates the scheduling of multi-purpose gates in a Haditha dam is publicly available in the repository: https://zenodo.org/records/23263653 (accessed on 1 September 2026).

**Conflicts of Interest:** The authors declare no conflicts of interest.

## Abbreviations

The following abbreviations are used in this manuscript:

| | |
| --- | --- |
| LSTM | Long Short-Term Memory |
| HHO | Harris Hawks Optimization |
| IMOHHO | Improved Harris Hawks Multi-Objective Algorithm |
| RMSE | Root Mean Square Error |

| | |
|---|---|
| MAE | Mean Absolute Error |
| $R^2$ | Coefficient Of Determination |
| DER | Distributed Energy Resource |
| ANN | Artificial Neural Network |
| RNN | Recurrent Neural Network |
| EMS | Energy Management System |
| GA | Genetic Algorithm |
| WOA | Whale Optimization Algorithm |
| DRL | Deep Reinforcement Learning |
| MARL | Multi-Agent Reinforcement Learning |
| RL | Reinforcement Learning |

## References


1. Priyanka, M.; Ghanshyam, S. Energy management systems in sustainable smart cities based on the internet of energy: A technical review. *Energies* **2023**, *16*, 6903. [CrossRef]
2. George, Z.; Mansour, A.; Pinhas, A.; Philippe, C.; Wolfgang, C.; Dahdal, Y.; Fnais, M.; Francis, D.; Hadjinicolaou, P.; Howari, F.; et al. Climate change and weather extremes in the Eastern Mediterranean and Middle East. *Rev. Geophys.* **2022**, *60*, e2021RG000762. [CrossRef]
3. Pomoni, D.I.; Koukou, M.K.; Vrachopoulos, M.G.; Vasiliadis, L. A review of hydroponics and conventional agriculture based on energy and water consumption, environmental impact, and land use. *Energies* **2023**, *16*, 1690. [CrossRef]
4. Chowdhury, A.K.; Wild, T.; Zhang, Y.; Binsted, M.; Iyer, G.; Kim, S.H.; Lamontagne, J. Hydropower expansion in eco-sensitive river basins under global energy-economic change. *Nat. Sustain.* **2024**, *7*, 213–222. [CrossRef]
5. Yang, Y.; David, T.; Zhenong, J.; Pete, S.; Christopher, B.; Yong-Guan, Z.; Jennifer, B.; Paolo, D.; Peter, F.; Joe, F.; et al. Climate change exacerbates the environmental impacts of agriculture. *Science* **2024**, *385*, eadn3747. [CrossRef] [PubMed]
6. Ateyah, A.; Ageel, A.; Saad, A.; Khaled, A. The role of smart infrastructure in residential water demand management: A global survey. *Water* **2025**, *17*, 3119. [CrossRef]
7. Deepali, U.; Abhishek, K.; Inderjeet, B.; Ashutosh, S.; Mayank, G.; Prashant, K. Balancing act: Water resource management in the face of floods, droughts, and extreme weather events. In *Advances in Hydrology*; Elsevier: Amsterdam, The Netherlands, 2026; pp. 209–222. [CrossRef]
8. Hill, G.M. Reinventing Systems in the Utilities Industry. *J. Syst. Manag.* **1992**, *43*, 23.
9. Memon, M.M.; Halepoto, I.A.; Abro, M.A.J.; Khuhawar, F.Y. Distributed energy storage systems for distributed energy resources integration. In *Distributed Energy Storage Systems for Digital Power Systems*; Elsevier: Amsterdam, The Netherlands, 2025; pp. 319–358. [CrossRef]
10. Islam, M.M.; Yu, T.; Giannoccaro, G.; Mi, Y.; La Scala, M.; Nasab, M.R.; Wang, J. Improving reliability and stability of the power systems: A comprehensive review on the role of energy storage systems to enhance flexibility. *IEEE Access* **2024**, *12*, 152738–152765. [CrossRef]
11. Parzen, M.; Neumann, F.; Van Der Weijde, A.H.; Friedrich, D.; Kiprakis, A. Beyond cost reduction: Improving the value of energy storage in electricity systems. *Carbon Neutrality* **2022**, *1*, 26. [CrossRef]
12. Xu, J.; Zheng, T.; Dang, Y.; Yang, F.; Li, D. Distributed deep reinforcement learning for data-driven water heater model in smart grid. *IEEE Trans. Smart Grid* **2025**, *16*, 2900–2912. [CrossRef]
13. Hossain, M.E.; Tarafder, M.T.R.; Ahmed, N.; Al Noman, A.; Sarkar, M.I.; Hossain, Z. Integrating AI with edge computing and cloud services for real-time data processing and decision making. *Int. J. Multidiscip. Sci. Arts* **2023**, *2*, 252–261. [CrossRef]
14. Yatsenko, D.V.; Popov, V.A.; Rozen, V.P.; Zamulko, A.I.; Adanikov, O.V. Accounting the factor of randomity of social processes in prediction of demand for electric energy. *Natsional'Nyi Hirnychyi Universytet Nauk. Visnyk* **2022**, *2*, 67–72. [CrossRef]
15. Mansouri, M.; Safavi, H.R.; Rezaei, F. An improved MOPSO algorithm for multi-objective optimization of reservoir operation under climate change. *Environ. Monit. Assess.* **2022**, *194*, 261. [CrossRef] [PubMed]
16. Ali, Z.M.; Calasan, M.; Aleem, S.H.A.; Jurado, F.; Gandoman, F.H. Applications of energy storage systems in enhancing energy management and access in microgrids: A review. *Energies* **2023**, *16*, 5930. [CrossRef]
17. Young, G.K., Jr. Finding reservoir operating rules. *J. Hydraul. Div.* **1967**, *93*, 297–322. [CrossRef]
18. Stedinger, J.R.; Sule, B.F.; Loucks, D.P. Stochastic dynamic programming models for reservoir operation optimization. *Water Resour. Res.* **1984**, *20*, 1499–1505. [CrossRef]
19. Yeh, W.W.-G. Reservoir management and operations models: A state-of-the-art review. *Water Resour. Res.* **1985**, *21*, 1797–1818. [CrossRef]

20. Labadie, J.W. Optimal operation of multireservoir systems: State-of-the-art review. *J. Water Resour. Plan. Manag.* **2004**, *130*, 93–111. [CrossRef]
21. Takeuchi, K. *Sustainable Reservoir Development and Management*; International Association of Hydrological Sciences: Oxfordshire, UK, 1998.
22. Sierra Nevada Ecosystem Project and SNEP Science Team and University of California (System); Centers for Water and Wildland Resources. *Sierra Nevada Ecosystem Project Final Report to Congress: Status of the Sierra Nevada*; Centers for Water and Wildl Ornia: Sacramento, CA, USA, 1996; Volume 2.
23. Hansamali, U.; Makumbura, R.K.; Rathnayake, U.; Azamathulla, H.M.; Muttil, N. Leaky dams as nature-based solutions in flood management Part I: Introduction and comparative efficacy with conventional flood control infrastructure. *Hydrology* **2025**, *12*, 95. [CrossRef]
24. Sseguya, F.; Jun, K.S. Deep Reinforcement Learning for Optimized Reservoir Operation and Flood Risk Mitigation. *Water* **2025**, *17*, 3226. [CrossRef]
25. Gomes, M.A.; Meisen, T. A review on customer segmentation methods for personalized customer targeting in e-commerce use cases. *Inf. Syst. e-Bus. Manag.* **2023**, *21*, 527–570. [CrossRef]
26. Egner, T. Principles of cognitive control over task focus and task switching. *Nat. Rev. Psychol.* **2023**, *2*, 702–714. [CrossRef] [PubMed]
27. Massaoudi, M.S.; Abu-Rub, H.; Ghrayeb, A. Navigating the landscape of deep reinforcement learning for power system stability control: A review. *IEEE Access* **2023**, *11*, 134298–134317. [CrossRef]
28. Alvi, I.A.; Alvi, I.S. Why dams fail: A systems perspective and case study. *Civ. Eng. Environ. Syst.* **2023**, *40*, 150–175. [CrossRef]
29. Qiliang, W.; Nianwen, C.; Minghui, Y.; Yan, N.; Cong, W. Nonlinear dynamic analysis of FG fluid conveying micropipes with initial imperfections. *Int. J. Struct. Stab. Dyn.* **2025**, *25*, 2550017. [CrossRef]
30. Cea, L.; Costabile, P. Flood risk in urban areas: Modelling, management and adaptation to climate change. A review. *Hydrology* **2022**, *9*, 50. [CrossRef]
31. Alena, V.; Miroslav, G.; Ľuboslav, S. Selected mathematical optimization methods for solving problems of engineering practice. *Energies* **2022**, *15*, 2205. [CrossRef]
32. Swedan, N.H. Thermodynamic Analysis of Climate Change. *Entropy* **2023**, *25*, 72. [CrossRef] [PubMed]
33. Li, D.; Qi, Z.; Zhou, Y.; Elchalakani, M. Machine learning applications in building energy systems: Review and prospects. *Buildings* **2025**, *15*, 648. [CrossRef]
34. Grygier, J.C.; Stedinger, J.R. Algorithms for optimizing hydropower system operation. *Water Resour. Res.* **1985**, *21*, 1–10. [CrossRef]
35. Bhanu, C.; Kumaravelan, G. Integration of artificial intelligence techniques for energy management. In *Sustainable Management of Electronic Waste*; Wiley: Hoboken, NJ, USA, 2024; pp. 1–46. [CrossRef]
36. Alharbi, S. Integrating neural forecasting with multi-objective optimization for sustainable EV infrastructure in smart cities. *Sustainability* **2025**, *17*, 9342. [CrossRef]
37. UKingsley, K.; Olatunji, K.O.; Eyitayo, A.; Tien-Chien, J.; Madyira, D.M. Optimizing renewable energy systems through artificial intelligence: Review and future prospects. *Energy Environ.* **2024**, *35*, 3833–3879. [CrossRef]
38. Andreas, E.; Demetris, K. One decade of multi-objective calibration approaches in hydrological modelling: A review. *Hydrol. Sci. J.–J. Des. Sci. Hydrol.* **2010**, *55*, 58–78. [CrossRef]
39. Yuhui, W.; Xiaohui, L.; Yunzhong, J.; Hao, W. Performance comparison of three multi-objective optimization algorithms on calibration of hydrological model. In *Proceedings of the 2010 Sixth International Conference on Natural Computation*; IEEE: New York, NY, USA, 2010; Volume 6, pp. 2798–2803.
40. Hamid, G.; Masoud, A.; Tricia, S.; Phoebe, R.; Habtamu, T. Integrated water resources and hydropower generation modelling in a complex, cold-regions river-reservoir system. *Sustain. Water Resour. Manag.* **2026**, *12*, 20. [CrossRef]
41. Amer, S.; Qian, Z.; Alessandro, R.; Ahmed, M.; Badr, A.; Omar, A.; Kumar, M.M.; Yongqiang, Q. A novel GA-LSTM method for water flow prediction with real climate data. In *Proceedings of the 2026 1st International Conference on Emerging Trends in Advancements and Applications of Computational Intelligence Techniques (ETAACT)*; IEEE: New York, NY, USA, 2026; pp. 1–6. [CrossRef]
42. Mowafaq, I.A.; Abdullah, S.S.; Hoobi, I.R. Evaluation of Seepage on the Right Side of Haditha Dam, West of Iraq. In *Proceedings of the IOP Conference Series: Earth and Environmental Science*; IOP Publishing: Bristol, UK, 2022; Volume 1080, p. 012012. [CrossRef]
43. Zafar, K.S.; Nazeefa, M.; Salman, G.; Haibat, K.; Hasan, Z.S.M.; Jeza, A.A.; Imran, A. Quantum long short-term memory (QLSTM) vs. classical LSTM in time series forecasting: A comparative study in solar power forecasting. *Front. Phys.* **2024**, *12*, 1439180. [CrossRef]
44. Minotti, G. Cryptocurrencies Price Prediction Using LSTM Neural Network Model. Ph.D. Thesis, Università Ca' Foscari Venezia, Venice, Italy, 2023. [CrossRef]
45. Gharehchopogh, F.S. An improved Harris Hawks optimization algorithm with multi-strategy for community detection in social network. *J. Bionic Eng.* **2023**, *20*, 1175–1197. [CrossRef]

46. Alsokhiry, F. Leveraging Harris Hawks Optimization for enhanced multi-objective optimal power flow in complex power systems. *Energies* **2024**, *18*, 18. [CrossRef]
47. Yuehao, S.; Zhijun, Q. Detection, differentiation and localization of replay attack and false data injection attack based on random matrix. *Sci. Rep.* **2024**, *14*, 2758. [CrossRef] [PubMed]
48. Asghar, H.A.; Seyedali, M.; Hossam, F.; Ibrahim, A.; Majdi, M.; Huiling, C. Harris hawks optimization: Algorithm and applications. *Future Gener. Comput. Syst.* **2019**, *97*, 849–872. [CrossRef]
49. Amer, S.; Qian, Z.; Alessandro, R.; Ahmed, M.; Badr, A.; Omer, A.; Kumar, M.M.; Yongqiang, Q. Development of a new technique dam gates opening scheme based on Whale Optimization Algorithm with Long Short Term Memory (WOA-LSTM). In *2026 1st International Conference on Emerging Trends in Advancements and Applications of Computational Intelligence Techniques (ETAACT)*; IEEE: New York, NY, USA, 2026; pp. 1–6. [CrossRef]

**Disclaimer/Publisher's Note:** The statements, opinions and data contained in all publications are solely those of the individual author(s) and contributor(s) and not of MDPI and/or the editor(s). MDPI and/or the editor(s) disclaim responsibility for any injury to people or property resulting from any ideas, methods, instructions or products referred to in the content.